International Journal of Fracture **60**: 49–63, 1993.

Failure analysis of a cracked plate based on endochronic plastic theory coupled with damage

C.L. CHOW[1] and X.F. CHEN[2]
[1]*Department of Mechanical Engineering, The University of Michigan-Dearborn, Dearborn, Michigan 48128-1491, USA*
[2]*Department of Mechanical Engineering, University of Hong Kong, Pokfulam Road, Hong Kong*

Received 10 February 1992; accepted in revised form 17 September 1992

Abstract. An anisotropic model of damage mechanics for ductile fracture incorporating the endochronic theory of plasticity is presented in order to take into account material deterioration during plastic deformation. An alternative form of endochronic (internal time) theory which is actually an elasto-plastic damage theory with isotropic-nonlinear kinematic hardening is developed for ease of numerical computation. Based on this new damage model, a finite element algorithm is formulated and then employed to characterize the fracture of thin aluminum plate containing a center crack. A new criterion termed as Y_R-Criterion is proposed to define both the crack initiation angle and load. Experiments have been conducted to verify the validity of the proposed damage model and it is found that the theoretical crack initiation loads correspond closely with the measured values.

1. Introduction

The conventional fracture mechanics approach has been successfully applied to characterize fracture behavior of brittle materials by means of the global parameter K or G describing the threshold condition of crack initiation independent of a particular geometry and loading condition. For ductile materials where plastic deformation at the crack tip can no longer be ignored, the fracture parameters such as COD and J-integral are often employed, but their validity as a single global parameter to characterize the ductile fracture has been questioned, especially when the loading condition is complex [1–3]. For the global approach of fracture, the concept of process zone is introduced at the region where fracture process actually takes place. But the real process within this zone is left unresolved. Thus the application of J in fracture analysis requires that a J-dominance region exists in the crack tip and its size should be larger that that of the process zone. However, J-integral is only proven to be path independent within the deformation theory of plasticity. When the plastic deformation is extensive at the crack tip, the deformation theory of plasticity can no longer describe the material responses adequately under nonproportional loading. Since most engineering structures of practical importance are subjected to nonproportional loading conditions, the applicability of the J-integral as a single parameter in fracture analysis becomes questionable. Another important factor is the observed extensive material deterioration at the crack tip, and it is the material deterioration that accumulates within the process zone of the crack tip and causes the final macrocrack initiation and propagation that will be discussed later.

In reality, most engineering materials contain microcracks/microvoids which initiate and coalesce in the immediate vicinity of a macrocrack tip due to the development of large plastic deformation causing material deterioration/damage. Based on the concept of damage mechanics, the initiation, growth and coalescence of microcracks as a local phenomenon of material degradation will lead to crack initiation and finally, crack propagation of a

macrocrack. The damage evolution is considered as a process, dependent not only on the final stress state, but also on its history reminiscent of plastic deformation. In the fracture analysis with damage consideration, the macrocrack initiation and propagation resulting from the development of damage are progressive processes of damage accumulation which are also history dependent processes. For the local approach of fracture with damage consideration, damage criteria are employed for predicting microcrack initiation and propagation which are related to the actual material failure ahead of the crack tip, so that the crack tip fields of stress, strain, damage etc. should be evaluated precisely. This is achieved in the local approach of fracture by developing a constitutive equation coupled with damage. The stiffness change due to the existence of microdefects and thus redistribution of stress in the crack tip can be manifested in the analysis. The local fields of stress, strain and damage are precisely evaluated with the constitutive equation coupled with damage. Therefore the local approach of fracture can better characterize localized material behaviors within what is commonly known as the 'process zone' or 'characteristic length' where the precise stress and strain distributions are ignored or cannot be taken into account based on the conventional global approach of fracture mechanics.

The damage mechanics originated by Kachanov in 1958 [4] has been extensively studied during the past two decades [5–11]. This has led to successful characterization of particular problems in fatigue, creep fracture, creep-fatigue interaction and ductile fracture. As an example of its power in solving fracture problems, Chow et al. successfully characterized ductile fracture of thin aluminum plate containing a center crack [12, 13, 14] with a damage model incorporating classical plasticity theory. Recently, a damage model coupled with the endochronic plastic theory has been proposed by Chow and Chen [15]. The endochronic plastic theory first introduced by Valanis [16] contains an essential ingredient known as intrinsic time, which is dependent on the material properties and deformation history and is used to describe the history-dependent mechanical response. And the classical plastic theory can be deduced as a special case of endochronic theory. For the endochronic theory coupled with damage [15], the damage variable introduced is an internal state variable based on the irreversible thermodynamics. The equation of damage evolution derived is obtained by the orthogonality rule from a dissipation power where a new intrinsic time is introduced in addition to the conventional intrinsic time because the damage mechanism is different from the mechanism of plastic response.

The distributions of stress, strain/plastic strain and damage are not in general uniform in practical engineering structures of arbitrary geometry with random service loading conditions. Due to the complexity of constitutive equations and boundary conditions, obtaining analytic solutions for these structures is often difficult if not impossible to achieve. In this paper, a finite element formulation for the endochronic theory coupled with damage is developed and then employed to analyze the stress, strain and damage distributions of a plate with a center macrocrack. In addition, another important object of this paper is to check the validity of the endochronic theory coupled with damage for a typical engineering structure subject to complex loading conditions other than simple tension as described in our earlier publication [15]. This requires the development of two fracture criteria to determine the angle and the threshold condition of a macrocrack initiation respectively. The predicted crack initiation angle and fracture loads are then compared with those determined from experiments.

1.1. The endochronic (internal time) theory coupled with damage

For the endochronic theory coupled with damage, the intrinsic time measure and intrinsic time are evaluated from the effective plastic strain. Since the volume deformation is considered to be elastic, the effective differential strain tensor is expressed as $\mathrm{d}\tilde{\boldsymbol{\varepsilon}} = \mathrm{d}\tilde{\boldsymbol{\varepsilon}}^e + \mathrm{d}\tilde{\boldsymbol{\varepsilon}}^p = (\mathrm{d}\tilde{\mathbf{e}}^e + \mathrm{d}\tilde{\mathbf{e}}^p) + \mathbf{I}\,\mathrm{d}\tilde{\varepsilon}^e_m$. The intrinsic time measure is defined as

$$\mathrm{d}\zeta = (\mathrm{d}\tilde{\mathbf{e}}^p : \mathrm{d}\tilde{\mathbf{e}}^p)^{1/2} \tag{1.1}$$

and the intrinsic time is defined from the intrinsic time measure as

$$\mathrm{d}z = \frac{\mathrm{d}\zeta}{f(\zeta)}, \tag{1.2}$$

where $f(\zeta)$ is hardening or softening function respectively for hardening or softening material and its initial value is $f(0) = 1$. In [15], an endochronic plastic theory coupled with damage has been established from the irreversible thermodynamics where the damage variable is considered as an internal variable,

$$\tilde{\mathbf{S}} = 2\mu_0 \int_0^z \rho(z - z') \frac{\partial \tilde{\mathbf{e}}^p}{\partial z'} \mathrm{d}z', \tag{1.3}$$

where $\tilde{\mathbf{S}}$ is the deviatoric part of effective stress, $\tilde{\mathbf{e}}^p$ is the effective deviatoric plastic strain, which is equal to the effective plastic strain due to the plastic incompressibility

$$\tilde{\mathbf{S}} = \tilde{\boldsymbol{\sigma}} - \frac{\tilde{\boldsymbol{\sigma}}_m}{3}\mathbf{I}, \tag{1.4}$$

where $\tilde{\boldsymbol{\sigma}}_m = \tilde{\boldsymbol{\sigma}}_{kk}$ and the effective stress is

$$\tilde{\boldsymbol{\sigma}} = \mathbf{M}(\mathbf{D}) : \sigma. \tag{1.5}$$

The elastic constitutive equation is assumed to be

$$\tilde{\boldsymbol{\sigma}} = \mathbf{E} : \tilde{\boldsymbol{\varepsilon}}^e, \tag{1.6}$$

which is similar in form to the conventional elastic constitutive equation, and $\mathbf{E}$ is the elastic stiffness tensor. The kernel function is chosen as $\rho(z) = \sum_{r=1}^{n} a_r \mathrm{e}^{-\beta_r Z}$ and β_1 is of large enough order to describe the weak singularity of $\rho(z)$, and an endochronic plastic theory coupled with damage is thus achieved, yielding satisfactory agreement between those predicted and determined experimentally [15].

Watanabe et al. proposed a modified form of endochronic theory by assuming $\rho(z) = \rho_0 \delta(z) + \rho_1(z)$, where $\delta(z)$ is Dirac delta function and $\rho_1(z)$ is a non-singular function [17].

Although the theory proposed by Watanabe et al. is accompanied with the yield surface due to the introduction of $\delta(z)$, yet it is not the same as classical plasticity theory, which may be obtained as a special case of the endochronic theory by carefully choosing $\rho_1(z)$ and $f(\zeta)$ [18]. The numerical implementation of the modified endochronic theory coupled with damage is similar to that of classical plastic theory.

For the present investigation, the form of $\rho(z)$ is retained

$$\rho(z) = \rho_0 \delta(z) + \rho_1(z), \tag{1.7}$$

where $\rho_1(z)$ is a non-singular function and is assumed to be of the form $\rho_1(z) = \sum_{r=1}^{n} C_r \, e^{-\alpha_r Z}$. Substituting the above equation into (1.3), we have

$$\tilde{\mathbf{S}} = S_y^0 \frac{d\tilde{\mathbf{e}}^p}{dz} + \mathbf{r}(z), \tag{1.8}$$

where

$$\mathbf{r}(z) = 2\mu_0 \int_0^z \rho_1(z - z') \frac{d\tilde{\mathbf{e}}^p}{dz'} dz' \tag{1.9}$$

and

$$S_y^0 = 2\mu_0 \rho_0. \tag{1.10}$$

The elastic and plastic regions are characterized by the following conditions:

(i) $\|\tilde{\mathbf{S}} - \mathbf{r}\| < S_y^0 f(\zeta)$ when the material is in the elastic region. (1.11)
(ii) $\|\tilde{\mathbf{S}} - \mathbf{r}\| = S_y^0 f(\zeta)$ when the material is elastically unloading.

$$(\tilde{\mathbf{S}} - \mathbf{r}) : d\tilde{\boldsymbol{\varepsilon}} \leqslant 0 \tag{1.12}$$

(iii) $\|\tilde{\mathbf{S}} - \mathbf{r}\| = S_y^0 f(\zeta)$ when plastic deformation is permissible.

$$(\tilde{\mathbf{S}} - \mathbf{r}) : d\tilde{\boldsymbol{\varepsilon}} > 0, \tag{1.13}$$

where $\mathbf{r}(z)$ is the 'back stress' as in classical plasticity theory, which describes the translation of the yield surface. The hardening function $f(\zeta)$ describes the dilatation of the yield surface. In endochronic theory, the evolution of $\mathbf{r}(z)$ is nonlinear and can be considered as a form of nonlinear kinematic hardening. Before the onset of damage, the material is assumed to be isotropic. With (1.4), (1.6) and (1.8), the incremental stress-strain relationship based on the endochronic plastic theory coupled with damage is obtained and is analogous in form to

the classical plasticity theory

$$d\tilde{\boldsymbol{\sigma}} = 2\mu_0(d\tilde{\boldsymbol{\varepsilon}} - d\tilde{\boldsymbol{\varepsilon}}^p) + \lambda_0(\mathbf{I}:d\tilde{\boldsymbol{\varepsilon}})\mathbf{I}$$

$$= 2\mu_0\, d\tilde{\boldsymbol{\varepsilon}} + \lambda_0(\mathbf{I}:d\tilde{\boldsymbol{\varepsilon}})\mathbf{I} - \frac{2\mu_0(\tilde{\mathbf{S}} - \mathbf{r})\langle(\tilde{\mathbf{S}} - \mathbf{r}):d\tilde{\mathbf{e}}\rangle}{C(S_y^0)^2 f^2(\zeta)}\Gamma, \tag{1.14}$$

where

$$C = 1 + \rho_1(0) + \frac{(\tilde{\mathbf{S}} - \mathbf{r}):\mathbf{h}^*}{S_y^0 f^2(\zeta)} + \frac{S_y^0 f'}{2\mu_0} \tag{1.15}$$

and

$$\mathbf{h}^* = \int_0^z \frac{d\rho_1}{dz}(z - z')\frac{d\tilde{\mathbf{e}}^p}{dz'}dz' \tag{1.16}$$

and $\Gamma = 1$ when condition (iii) is satisfied, i.e. plastic loading. $\Gamma = 0$ when condition (i) or (ii) holds, i.e. elastic or elastic unloading.

According to the definition of effective stress

$$\tilde{\boldsymbol{\sigma}}_{ij} = \mathbf{M}_{ijkl}(\mathbf{D})\sigma_{kl}$$

and the symmetric properties of $\tilde{\boldsymbol{\sigma}}$ and σ infer

$$\mathbf{M}_{ijkl} = \mathbf{M}_{jikl} = \mathbf{M}_{ijlk},$$

where $\mathbf{M}$ is a fourth order tensor and represents the effect of damage on stress. The question on the choice of the order of the damage tensor and the relationship between $\mathbf{M}$ and $\mathbf{D}$ is assumed to be [15]

$$\mathbf{M} = (\mathbf{I} - D)^{-1} \tag{1.17}$$

and

$$D_{ijkl} = \tfrac{1}{4}(\delta_{ik}D_{jl} + \delta_{il}D_{jk} + \delta_{jk}D_{il} + \delta_{jl}D_{ik}). \tag{1.18}$$

Following the conventional choice in damage mechanics, a symmetric tensor $\mathbf{D}$ of order two is employed. As for a symmetric tensor of order two, there exist three principal axes. In the principal coordinate system, the damage tensor $\mathbf{D}$ may be represented by

$$\mathbf{D} = \begin{bmatrix} D_1 & 0 & 0 \\ & D_2 & 0 \\ \mathbf{S} & & D_3 \end{bmatrix}. \tag{1.19}$$

Due to symmetry, **M(D)** may be written in a 6 × 6 matrix form, and its relation to **D** is chosen as the following form. In the principal coordinate system [15]

$$[\mathbf{M(D)}] = \begin{bmatrix} \frac{1}{1-D_1} & & & & & \\ & \frac{1}{1-D_2} & & & 0 & \\ & & \frac{1}{1-D_3} & & & \\ & & & \frac{2}{2-(D_2+D_3)} & & \\ & 0 & & & \frac{2}{2-(D_1+D_3)} & \\ & & & & & \frac{2}{2-(D_1+D_2)} \end{bmatrix}. \tag{1.20}$$

For an arbitrary coordinate system, **M(D)** can be easily deduced through tensor transformation.

The ductile damage evolves only when the plastic deformation occurs. Therefore it is more appropriate to use the intrinsic time scale to describe damage evolution rather than the commonly used time scale. The intrinsic time scale introduced before is however not applicable to the description of damage evolution because the mechanics of damage evolution is different. A new intrinsic time scale is therefore introduced as

$$\mathrm{d}z_d = f_{tr}(\tilde{\sigma})\,\mathrm{d}\zeta / f_d(\zeta), \tag{1.21}$$

where subscript d represents the effects on damage evolution. The main reason that the intrinsic time measure ζ is adopted here is that the evolution of ductile damage is closely related to plastic deformation and ζ is a measure in the plastic strain space. Also the damage is dependent on the stress state, the effect of stress triaxiality on damage evolution is introduced by the function $f_{tr}(\tilde{\sigma})$.

Damage evolution is a dissipative process based on the irreversible thermodynamics. In what follows, the relationship between the damage evolution and damage dissipation is established. If the damage dissipation is not coupled with mechanical dissipation, the damage dissipation 'power' to z_d must satisfy the following dissipation inequality

$$\mathbf{Y} : \frac{\mathrm{d}\mathbf{D}}{\mathrm{d}z_d} = \Phi(\mathbf{Y}) \geqslant 0, \tag{1.22}$$

where Φ is the dissipation 'power'. **Y** is the damage strain energy release rate, the conjugate force to damage **D**, which is defined as [15]

$$\mathbf{Y} = \sigma : \left[\tilde{\mathbf{E}}^{-1} : \mathbf{M}^{-1}(\mathbf{D}) : \frac{\partial \mathbf{M}(\mathbf{D})}{\partial \mathbf{D}} \right]^s : \sigma. \tag{1.23}$$

From (1.17), we have

$$\frac{\partial \mathbf{M}(\mathbf{D})}{\partial \mathbf{D}} = \frac{\partial (1-D)^{-1}}{\partial \mathbf{D}} = \mathbf{M}(\mathbf{D}) : \frac{\partial D}{\partial \mathbf{D}} : \mathbf{M}(\mathbf{D}). \tag{1.24}$$

Using the relation (1.18), $\mathbf{Y}$ can be calculated from (1.23). As Voigt's notation for $\mathbf{Y}$ is employed, $\mathbf{Y}$ is represented by a vector $\{Y\}$. In the principal coordinate system of damage, the components of $\{Y\}$ are

$$Y_1 = \frac{1}{E}\left(\frac{\sigma_1^2}{V_{11}^3} - \frac{\nu\sigma_1\sigma_2}{V_{11}^2 V_{22}} - \frac{\nu\sigma_1\sigma_3}{V_{11}^2 V_{33}} + \frac{(1+\nu)\sigma_5^2}{V_{31}^3} + \frac{(1+\nu)\sigma_6^2}{V_{12}^3}\right), \tag{1.25}$$

$$Y_2 = \frac{1}{E}\left(-\frac{\nu\sigma_2\sigma_1}{V_{22}^2 V_{11}} + \frac{\sigma_2^2}{V_{22}^3} - \frac{\nu\sigma_2\sigma_3}{V_{22}^2 V_{33}} + \frac{(1+\nu)\sigma_4^2}{V_{23}^3} + \frac{(1+\nu)\sigma_6^2}{V_{12}^3}\right), \tag{1.26}$$

$$Y_3 = \frac{1}{E}\left(-\frac{\nu\sigma_1\sigma_3}{V_{33}^2 V_{11}} - \frac{\nu\sigma_3\sigma_2}{V_{33}^2 V_{22}} + \frac{\sigma_3^2}{V_{33}^3} + \frac{(1+\nu)\sigma_4^2}{V_{23}^3} + \frac{(1+\nu)\sigma_5^2}{V_{31}^2}\right), \tag{1.27}$$

$$\begin{aligned} Y_4 = \frac{1}{2E}\Bigg[&\left(-\frac{\nu}{V_{11}V_{22}V_{23}} - \frac{\nu}{V_{11}V_{33}V_{23}}\right)\sigma_1\sigma_4 + \left(\frac{1}{V_{22}^2 V_{23}} - \frac{\nu}{V_{22}V_{33}V_{23}}\right)\sigma_2\sigma_4 \\ &+ \left(\frac{1}{V_{33}^2 V_{23}} - \frac{\nu}{V_{22}V_{33}V_{23}}\right)\sigma_3\sigma_4 + \frac{1+\nu}{V_{23}^2 V_{22}}\sigma_2\sigma_4 + \frac{1+\nu}{V_{23}^2 V_{33}}\sigma_3\sigma_4 \\ &+ \frac{1+\nu}{V_{31}^2 V_{12}}\sigma_5\sigma_6 + \frac{1+\nu}{V_{12}^2 V_{31}}\sigma_5\sigma_6\Bigg], \end{aligned} \tag{1.28}$$

$$\begin{aligned} Y_5 = \frac{1}{2E}\Bigg[&\left(\frac{1}{V_{11}^2 V_{31}} - \frac{\nu}{V_{11}V_{33}V_{31}}\right)\sigma_1\sigma_5 + \left(-\frac{\nu}{V_{11}V_{22}V_{31}} - \frac{\nu}{V_{22}V_{33}V_{31}}\right)\sigma_2\sigma_5 \\ &+ \left(\frac{1}{V_{33}^2 V_{31}} - \frac{\nu}{V_{11}V_{33}V_{31}}\right)\sigma_3\sigma_5 + \frac{1+\nu}{V_{23}^2 V_{12}}\sigma_6\sigma_4 + \frac{1+\nu}{V_{12}^2 V_{23}}\sigma_6\sigma_4 \\ &+ \frac{1+\nu}{V_{31}^2 V_{11}}\sigma_5\sigma_1 + \frac{1+\nu}{V_{31}^2 V_{33}}\sigma_5\sigma_3\Bigg], \end{aligned} \tag{1.29}$$

$$\begin{aligned} Y_6 = \frac{1}{2E}\Bigg[&\left(\frac{\nu}{V_{11}^2 V_{22}} - \frac{\nu}{V_{11}V_{22}V_{12}}\right)\sigma_1\sigma_6 + \left(\frac{1}{V_{22}^2 V_{12}} - \frac{\nu}{V_{22}V_{11}V_{12}}\right)\sigma_2\sigma_6 \\ &+ \left(\frac{\nu}{V_{11}V_{33}V_{23}} - \frac{\nu}{V_{22}V_{33}V_{12}}\right)\sigma_3\sigma_6 + \frac{1+\nu}{V_{23}^2 V_{31}}\sigma_5\sigma_4 + \frac{1+\nu}{V_{31}^2 V_{23}}\sigma_5\sigma_4 \\ &+ \frac{1+\nu}{V_{12}^2 V_{11}}\sigma_1\sigma_6 + \frac{1+\nu}{V_{12}^2 V_{23}}\sigma_1\sigma_6\Bigg]. \end{aligned} \tag{1.30}$$

From the above equations, it is easy to observe that Y_4, Y_5, Y_6 are not equal to zero in the principal coordinate system of damage provided the principal coordinate systems of damage and stress are not coincident.

In an arbitrary coordinate system, $\mathbf{Y}$ can be easily obtained from the tensor transformation law. Then, from the orthogonality rule for dissipative process, the damage evolution equation is deduced as

$$\frac{\mathrm{d}\mathbf{D}}{\mathrm{d}z_d} = \frac{\mathbf{J}:\mathbf{Y}}{2(\frac{1}{2}\mathbf{Y}:\mathbf{J}:\mathbf{Y})^{1/2}}, \tag{1.31}$$

where

$$\Phi = [\tfrac{1}{2}\mathbf{Y}:\mathbf{J}:\mathbf{Y}]^{1/2}. \tag{1.32}$$

For the threshold condition of damage evolution z_d^0, (1.31) may be expressed alternatively as

$$\frac{\mathrm{d}\mathbf{D}}{\mathrm{d}z_d} = \frac{\lambda_d \mathbf{J}:\mathbf{Y}}{2(\frac{1}{2}\mathbf{Y}:\mathbf{J}:\mathbf{Y})^{1/2}} H(z_d - z_d^0), \tag{1.33}$$

where

$$H(z) = 1 \quad \text{for } z > 0,$$
$$H(z) = 0 \quad \text{for } z \leqslant 0$$

and

$$\lambda_d = \begin{cases} 1 & \text{when } \Phi = \Phi_{\max} \text{ and } \dfrac{\partial \Phi}{\partial \mathbf{Y}}:\mathrm{d}\mathbf{Y} > 0 \\ 0 & \text{when } \Phi < \Phi_{\max} \text{ or } \Phi = \Phi_{\max} \text{ and } \dfrac{\partial \Phi}{\partial \mathbf{Y}}:\mathrm{d}\mathbf{Y} \leqslant 0 \end{cases},$$

where $\Phi_{\max}$ is the maximum value of Φ.

According to (1.22) and (1.32), it can be shown that $\mathbf{J}$ must be a positive definite symmetric tensor

$$J_{ijkl} = J_{jikl} = J_{ijlk}$$

and we further assume that

$$J_{ijkl} = J_{klij}.$$

Because of the above symmetric properties, **J** may assume the following form [15]

$$\mathbf{J} = A\begin{bmatrix} 1 & \mu & \mu & & & & \\ & 1 & \mu & & & 0 & \\ & & 1 & & & & \\ & & & 2(1-\mu) & & & \\ & \mathbf{S} & & & 2(1-\mu) & & \\ & & & & & 2(1-\mu) & \end{bmatrix}. \tag{1.34}$$

2. The finite element formulation

With the development of the endochronic plastic constitutive equations coupled with damage and the damage evolution equations, the next step is to employ this damage model to characterize fracture in engineering structures under service loading. Generally numerical techniques are required to solve engineering problems of practical interest, because it is almost impractical to obtain an analytical solution due to the complexities of the constitutive equations involved and boundary conditions imposed. Since the finite element method has been shown to be a powerful numerical tool in engineering analysis, the method is therefore chosen to analyze the distributions of stress, strain and damage, and to predict the failure behavior of the structures.

The procedures in formulating the finite element analysis when damage is considered are similar in principle to the conventional FEM analysis, as the endochronic plastic constitutive equations are similar to the conventional plastic constitutive equations with isotropic–nonlinear kinematic hardening. Since the stiffness matrix [**K**] is expressed as a function of transformation [**B**] and the stress-strain matrix [**C**]

$$[\mathbf{K}] = \int_v [\mathbf{B}]^T[\mathbf{C}][\mathbf{B}]\,\mathrm{d}V, \tag{2.1}$$

where [**C**] is associated with the material properties while [**B**], with the element chosen for analysis, only [**C**] therefore needs to be modified in order to include the damage effects in the stiffness matrix. The effective elastic relation may be written in matrix form

$$\{\mathrm{d}\tilde{\sigma}\} = [\mathbf{C}^e]\{\mathrm{d}\tilde{\varepsilon}^e\}. \tag{2.2}$$

By incorporating the endochronic plastic constitutive equation (1.14) and the damage evolution equation, the above equation becomes

$$\{\mathrm{d}\tilde{\sigma}\} = [\mathbf{C}^*]\{\mathrm{d}\tilde{\boldsymbol{\varepsilon}}\}, \tag{2.3}$$

where

$$[\mathbf{C}^*] = [\mathbf{C}^e] - 2\mu_0 \frac{\{\hat{\mathbf{S}}\}\{\hat{\mathbf{S}}\}}{C(S_y^0)^2 f^2(\zeta)} \tag{2.4}$$

and $\hat{\mathbf{S}}$ denotes $(\tilde{\mathbf{S}} - \mathbf{r})$. Since $[\mathbf{C}]$ is the conventional real stress-strain matrix and $[\mathbf{C}^*]$ in (2.3) is the effective stress-strain matrix, it is desirable to transform (2.3) and express it in terms of the conventional real stress-strain matrix for ease of implementation with the finite element analysis. Equation (2.3) may thus be deduced as

$$\{d\sigma\} = [\tilde{\mathbf{C}}^*]\{d\varepsilon\}, \tag{2.5}$$

where

$$[\tilde{\mathbf{C}}^*] = [\mathbf{M}]([\mathbf{I}] - [\mathbf{Q}])([\mathbf{I}] + [\mathbf{C}^*][\mathbf{P}])^{-1}[\mathbf{C}^*][\mathbf{M}]^{T,-1}, \tag{2.6}$$

$$[\mathbf{Q}] = \lambda \frac{B_0}{f_d(\zeta)}[\mathbf{M}]\frac{\partial[\mathbf{M}]^{-1}}{\partial\{D\}^T}\frac{\partial\Phi}{\partial\{Y\}^T}[\mathbf{M}]\{\sigma\}\{\hat{\mathbf{S}}\}, \tag{2.7}$$

$$[\mathbf{P}] = \lambda \frac{B_0}{f_d(\zeta)}\frac{\partial[\mathbf{M}]^{T,-1}}{\partial\{D\}^T}\frac{\partial\Phi}{\partial\{Y\}^T}\{\varepsilon\}\{\hat{\mathbf{S}}\} \tag{2.8}$$

and

$$B_0 = \frac{1}{2\mu_0(C-1)S_Y^0 f(\zeta)}. \tag{2.9}$$

The material chosen for the present investigation is 2024-T3 aluminum alloy plate. The geometry of the specimen is shown in Fig. 1. Because of symmetry, only one quarter of the specimen needs to be analyzed, for which the finite element meshes are shown in Fig. 2 and Fig. 3. A total of 51 8-node elements resulting from 176 nodes are employed in the analysis and the elements are degenerated to radial elements at the crack tip in order to compute the radial and angular distribution of the physical quantities easily.

The first loading step chosen in the numerical analysis is relatively large up to when the onset of plastic deformation at the crack tip is observed. This is followed by the imposition of smaller load increments for the elasto-plastic analysis.

2.1. Experimental investigation

The test specimens whose geometry is shown in Fig. 1 are made of 2024-T3 aluminum alloy. A total of twelve specimens were manufactured, six each along the rolling and transverse direction so that the degree of material anisotropy, if any, may be examined.

A universal MTS testing machine was used to perform initial fatigue precracking at 10 Hz. An initial crack length of about 15 mm was formed at a load under which the maximum fatigue stress at the minimum cross section of specimens is less than half of the material yield stress of 330 MPa. A travelling microscope of 10X magnification was positioned close to the specimen for monitoring crack initiation.

The measured average load of crack initiation for all the specimens was 276.3 MPa. The average crack initiation load of the longitudinal specimens was slightly higher than that of the transverse specimens.

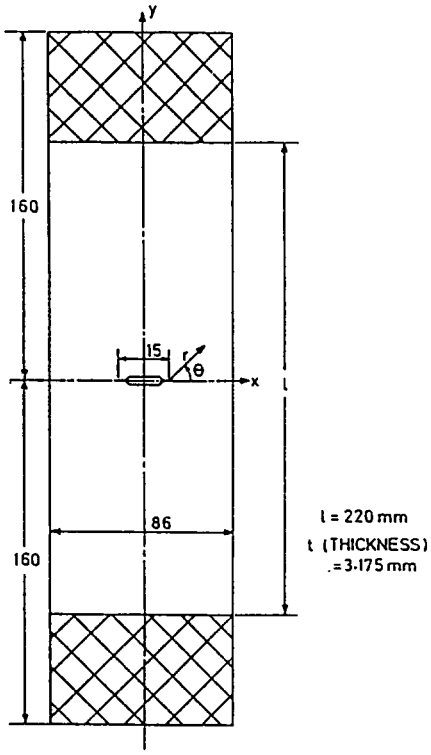

Fig. 1. The geometry of the specimen.

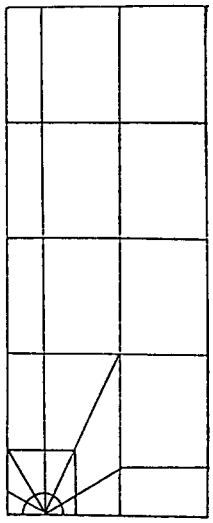

Fig. 2. The mesh for finite element analysis.

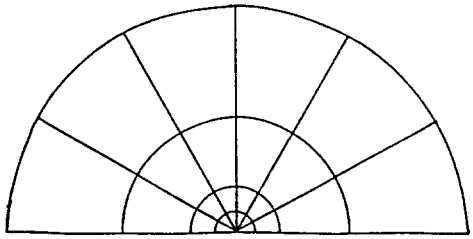

Fig. 3. The detailed finite element mesh near the crack tip.

3. Discussion of results

In order to provide a generalized solution in an engineering structure containing an embedded macrocrack, two criteria, namely the criterion governing the threshold condition of crack initiation and another one governing the determination of crack initiation angle must be developed.

The fracture criterion governing the determination of crack initiation angle has been the subject of intensive studies by many other investigators within the framework of fracture mechanics [19, 20]. In view of the development of a new plane known as the 'damage plane' hitherto not confronted in the conventional stress analysis, Wang and Chow [14] introduced a new fracture criterion known as the δ-criterion which was defined as the angle between the radial and principal damage planes in a material element. This is based on the physical consideration that the direction of crack initiation should be parallel to the plane of maximum

damage or the least δ-value between the principal damage and radial planes in an element ahead of the crack tip shown in Fig. 4.

With the determination of the angle of crack initiation using the δ-criterion, another criterion is required to characterize the threshold condition of crack initiation. From physical considerations, the threshold condition of crack initiation may be postulated to satisfy

$$W_D = \int_0^{\zeta} \mathbf{Y} : \mathrm{d}\mathbf{D}, \tag{3.1}$$

which attains its critical value in the crack initiation direction determined by δ-criterion.

The predicted δ-values at the material elements of various radical distributions are plotted against their corresponding angular positions as shown in Fig. 5. It can be readily observed from this figure that the predicted angle of crack initiation is zero degree, which agrees with the experimental observation.

Figure 6 depicts the angular distribution of the computed W_D values at different distances r from the crack tip. The uniform load applied on the specimen boundary causing crack initiation along the direction of $\delta = 0^\circ$ when the failure criterion $W_D = W_C$ is satisfied at $r_c = 0.07$ mm, is found to be 266 MPa. The measured W_C-value is 450×10^3 Pa. The predicted crack initiation load compares favorably with the experimentally determined average load of 276.3 MPa from 12 test specimens.

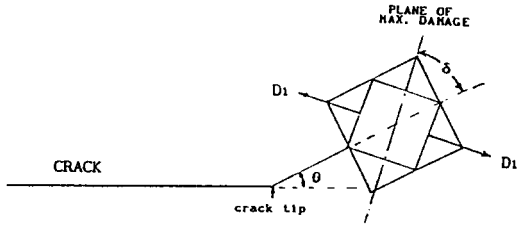

Fig. 4. The definition of δ near the crack tip.

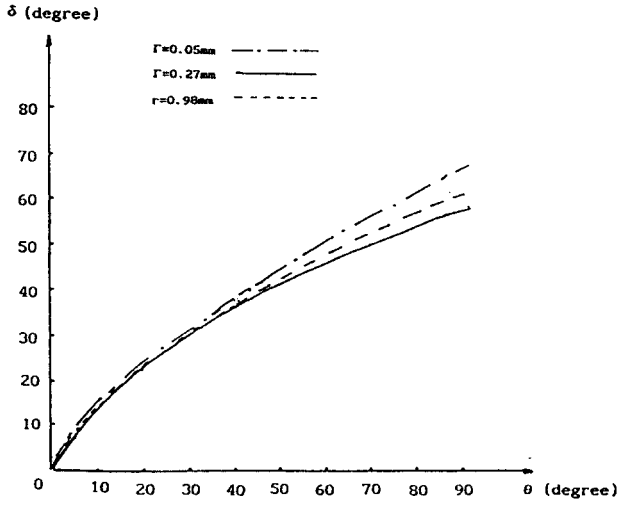

Fig. 5. δ vs. θ in the crack tip for different r.

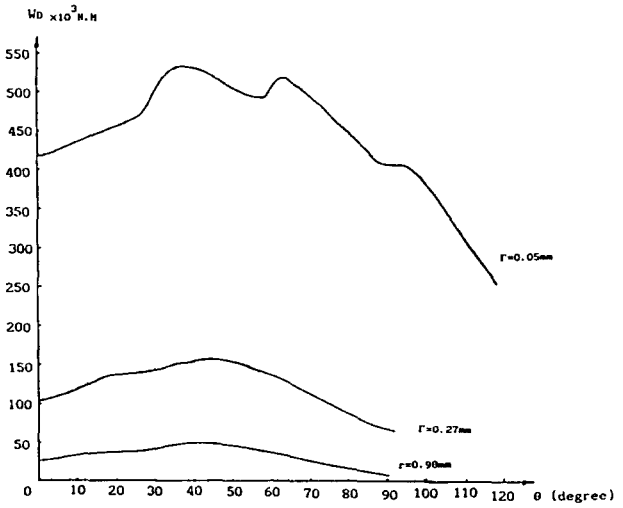

Fig. 6. W_D vs. θ in the crack tip for different r.

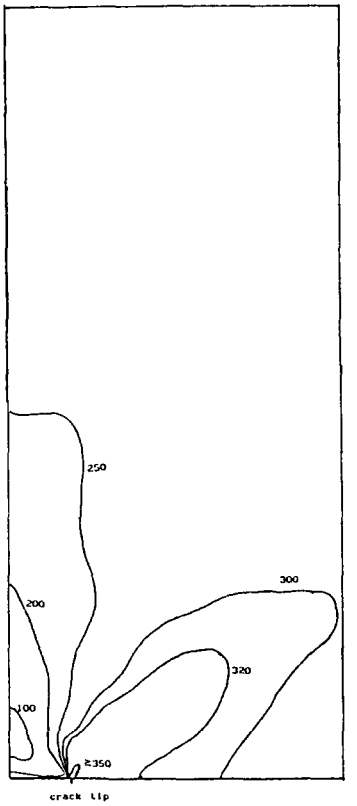

Fig. 7. The effective plastic equivalent stress $\tilde{\sigma}_p$ contour in the specimen.

Figure 7 depicts the computed effective plastic equivalent stress ($\tilde{\sigma}_p = \|\tilde{\mathbf{S}} - \mathbf{r}\|$) contours of the cracked specimens and Fig. 8, the detailed $\tilde{\sigma}_p$-contours at the crack tip when the applied load is 266 MPa. It can be observed from the figure that the maximum plastic deformation occurs, as expected, at about 45° to the crack line.

In addition to the W_D-fracture criterion, an alternative criterion of crack initiation based on the damage strain energy release rate $\mathbf{Y}$ shown in (1.25)–(1.30) and known as Y_R is defined as the tangential component of $\mathbf{Y}$ in a material element located at a particular radius from the crack tip as illustrated in Fig. 9. The threshold condition of crack initiation is postulated having been

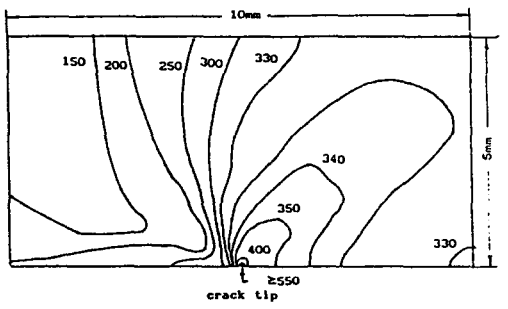

Fig. 8. The detailed $\tilde{\sigma}_p$ contour near the crack tip.

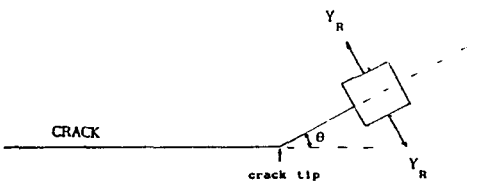

Fig. 9. The definition of Y_R near the crack tip.

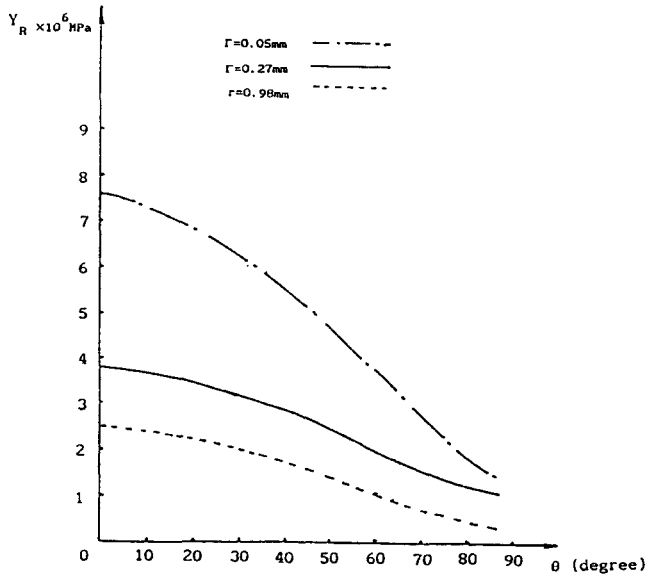

Fig. 10. Y_R vs. θ near the crack tip for different r.

satisfied along the θ-direction where the maximum Y_R at the particular radial distance attains the critical value of Y_C measured from a standard tensile specimen. Figure 10 illustrates the angular distribution of Y_R at the distance of 0.07 mm, 0.22 mm and 0.87 mm from the crack tip. It is evident from the figure that the maximum Y_R is located at the $\theta = 0°$ which agrees with the direction of crack propagation in a cracked specimen shown in Fig. 1 which exhibits a typical mode I failure. From the finite element analysis, the applied load that causes the maximum Y_R to attain the measured Y-value of 7.76 MPa at $r = 0.07$ mm is found to be 284 MPa which compares satisfactorily with the measured value of 276.3 MPa.

4. Conclusions

In this paper, an anisotropic model of damage mechanics incorporating the endochronic theory of plasticity for ductile fracture is developed and employed to characterize the angle of crack initiation and the threshold condition of crack initiation in thin aluminum plates containing an isolated crack. This is achieved by implementing the model into a finite element programme.

In addition to the δ-criterion for the determination of crack initiation angle and W_D-criterion for crack initiation load developed earlier by Chow and Wang [12], an alternative criterion of Y_R is introduced for the determination of both crack initiation angle and load. The fracture loads predicted based on the W_D-criterion and the Y_R-criterion were found to be respectively 266 MPa and 284 MPa which compared well with the measured value of 276.3 MPa.

Acknowledgement

The authors gratefully acknowledge the discussion with Dr. B.J. Duggan, Department of Mechanical Engineering, University of Hong Kong.

References

1. J.H. Giovanola and I. Finnie, *S. M. Archives* 9 (1984) 197–225.
2. J.H. Giovanola and I. Finnie, *S. N. Archives* 9 (1984) 227–257.
3. H.W. Liu and Tao Zhuang, *International Journal of Fracture* 27 (1985) R87–91.
4. L.M. Kachanov, *Izvestiya AN. SSSR., OTN.* (1958) 337–360.
5. J.P. Cordebois and F. Sidoroff, Colloque Euromech 115, Villard de Lans, June, 1979.
6. J.P. Codebois, Critères d'instabilite plastique et endommagement ductile en grand deformation, Thèse pour Doctorat d'Etat, Paris VI, May 1983.
7. Hao Lee et al., *Engineering Fracture Mechanics* 21 (1985) 1031–1054.
8. C.L. Chow and J. Wang, *Engineering Fracture Mechanics* 27 (1987) 547–558.
9. D. Krajcinovic et al., *Journal of Applied Mechanics* 48 (1981) 809–824.
10. F.A. Leckie et al., in *IUTAM Colloquium on Physical Nonlinearities in Structural Analysis* (1981) 140–155.
11. S. Murakami et al., *IUTAM Symposium on Creep in Structures* (1981) 422–444.
12. C.L. Chow and J. Wang, *Engineering Fracture Mechanics* 30 (1988) 547–563.
13. J. Wang and C.L. Chow, *Engineering Fracture Mechanics* 33 (1989) 309–317.
14. J. Wang and C.L. Chow, *Engineering Fracture Mechanics* 34 (1989) 209–220.
15. C.L. Chow and X.F. Chen, *International Journal of Fracture* 55 (1992) 115–130.
16. K.C. Valanis, *Archives of Mechanics* 23 (1971) 517–533.
17. O. Watanabe and S.N. Atluri, *Journal of Applied Mechanics* ASME 52 (1985) 857–866.
18. O. Watanabe and S.N. Atluri, *International Journal of Plasticity* 2 (1986) 37–57.
19. P.S. Theocaris and N.P. Andrionopoulos, *Engineering Fracture Mechanics* 16 (1983) 425–432.
20. G.C. Sih and E. Madenci, *Engineering Fracture Mechanics* 18 (1983) 667–677.
21. H.W. Liu, *Engineering Fracture Mechanics* 17 (1983) 425–438.
22. R.M. McMeeking and D.M. Parks, in *Elastic–Plastic Fracture, ASTM STP 668*, J.D. Landes, J.A. Begley, and G.A. Clarke (eds.), (1979) 175–194.
23. C.F. Shih and M.D. German, *International Journal of Fracture* 17 (1981) 27–43.